Embedded Tumor Size Estimation using Projections Analysis of Smartphone-based Compression-induced Images

***Abstract*—Smartphone-based Compression-induced Imaging Scope emulates the human touch sensation and non-invasively estimates the size of breast tumors. We used the segmented area projection of the tactile images to estimate the size of the embedded tumor. The sizes of the tumors were estimated with less than 23% error on phantoms and *in vivo* human patients. Also, the size estimation accuracy improved by 59% from the previous 3D interpolation method.**

Keywords: tactile imaging, non-invasive, embedded object size quantification, smartphone

I. Introduction

According to a 2019 study, 1,762,450 new diagnoses of breast cancer are anticipated [1], and globally 2.09 million cases of death occurred in 2018 due to breast cancer [2]. Although breast cancer screening is regularly performed in the developed countries, there are many women left out of this process; especially in the developing countries and rural areas [2], [3]. The smartphone-based Compression-induced Imaging Scope (SCIS) is designed to quantify the mechanical properties of the breast lesions. The mechanical properties are used to classify benign and malignant tumors. SCIS is a revamped version of the tactile sensation imaging system [4]. In this paper, the lesion size is estimated based on the segmented tactile image area projection.

II. System Overview

SCIS is the tactile imaging system that uses a smartphone camera to capture the light reflection pattern generated by the sensing tip's deformation. See Figure 1. Then, the smartphone transfers the image to the remote data processing unit over the Cloud. From the central data processing unit, the tumor's size is computed and retrieved to the phone through the Cloud.

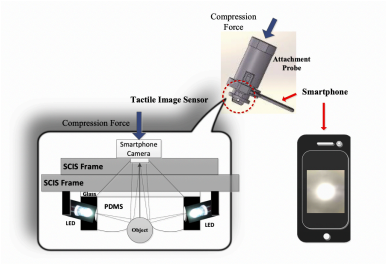

Figure 1. SCIS attachment probe and smartphone

The SCIS attachment probe includes four ultra-bright light emitting diodes (LEDs), a Polydimethylsiloxane (PDMS) sensing tip (20mm x 23mm x 14mm), a diffusion filter, a force sensor (FC22), and a controller circuit with wireless communication capability. The system measures the applied force corresponding to each image when the device is applied to the breast tissue's surface. The Bluetooth enabled microcontroller communicates with the smartphone to receive operator's input and to send the measured force value.

II. Segmented Area Projection Analysis

SCIS image has a relationship with the sensing tip deformation. As shown in Figure 2, we found the correlation between the diameter of a spherical inclusion and the segmented image's width and intensity value. SCIS images differ depending on the compression and the object's mechanical properties such as elasticity and shape. The optimal level of intensity is achieved when the applied force reaches above 20N.

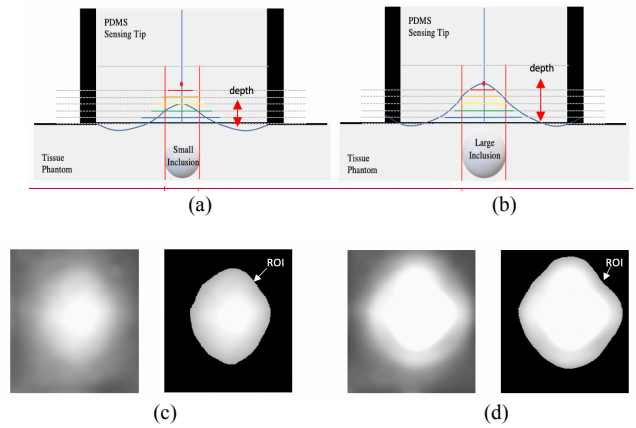

Figure 2. SCIS sensing tip deformation for (a) small (b) large inclusion and the corresponding region-of-interest (ROI) images (c) 8.8mm raw and segmented ROI and (d) 17.0mm raw and segmented ROI, generated by tissue compression with a hard and spherical shape inclusion

We use 1D projections of the SCIS images to analyze the image's pixel intensity and the light reflection pattern. In the previous study, we used the 3D interpolation model to estimate the size by developing four models based on the categories of the size of inclusion and the depth of tissue [5]. However, the estimated value highly fluctuates when we use the models on the SCIS images in the various conditions of elasticity and thickness of the tissue and inclusion. Based on the experiment and analysis, we found that segmentation improves the result of estimating size of an inclusion embedded of tissue from SCIS images. The adequate thresholding can reduce the error although the condition of inclusion and tissue changes. Moreover, there is a linear relationship between the size and the segmented image in the threshold. Thus, in this work, we introduce the projection analysis using the region-of-interest (ROI) segmentation, which allows us to recover the real size of the inclusion embedded within the tissue.

A. Segmentation using Intensity Thresholding

The threshold level is chosen based on the transition boundary where the light reflects with different angles depending on the tip's shape. In SCIS images, we can observe each pixel's intensity change when the strain of the

compressed tissue causes the tip's deformation. Due to the angle change of the light reflection inside the tip, pixels near the center of the image get brighter, and pixels toward the edge of the sensor get darker when the strain gets higher. We define the transition boundary from the intersection of uncompressed images and compressed images on a tissue. The transition boundary shown in Figure 3 was found at around 70% of the maximum intensity of images from the experimental data, and the intensity of the boundary is used as the thresholding intensity.

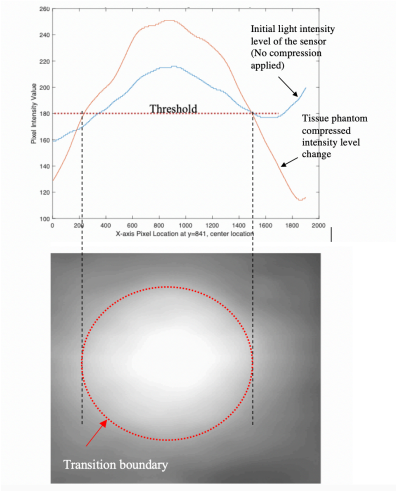

Figure 3. Transition boundary shown in 1D Intensity plot (top) on x-axis through the centroid of a SCIS example image (bottom: compressed tissue's image), plot without compression (blue line) and with compression (red line) for a tissue phantom.

B. *Projections of Segmented ROI*

As shown in Figure 4, we use projections at 0° and 90° angle due to the simplicity of the SCIS image that shows a symmetric peak located at the center in both x and y-direction as shown in Figure 4. We assume that the inclusion's shape is spherical and close to symmetric.

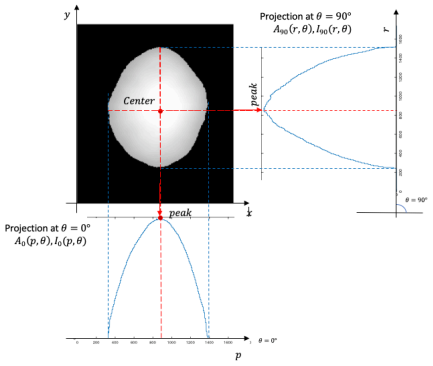

Figure 4. Segmented SCIS image's 0° and 90° angle projections that are the functions of p and r, the center of the image is indicated based on the area and intensity peaks' location of each projection

$$f_{bin}(x,y) = \begin{Bmatrix} 255, & if\ f(x,y) \geq Th \\ 0, & if\ f(x,y) < Th \end{Bmatrix} \quad (1)$$

$$f_{int}(x,y) = \begin{Bmatrix} f(x,y), & if\ f(x,y) \geq Th \\ 0, & if\ f(x,y) < Th \end{Bmatrix} \quad (2)$$

In (1), $f_{bin}(x,y)$ is the 0 and 255 pixel value at the location x and y that represents the result of image binarization to find the area of ROI. Unlikely, the function, $f_{int}(x,y)$ keeps the original pixel intensity value inside the segmented ROI. The 1D projection generated at the angle $\theta = 0°$ is based on the p-axis which corresponding to x-axis value. The projection at $\theta = 90°$ is projected based on r-axis which is corresponding to the value on y-axis as shown in Figure 4.

$$A_0(p,\theta) = \sum_{y=1}^{n} f_{bin}(x,y), \{when\ x = p\} \quad (3)$$

$$A_{90}(r,\theta) = \sum_{x=1}^{m} f_{bin}(x,y), \{when\ y = r\} \quad (4)$$

$$I_0(p,\theta) = \sum_{y=1}^{n} f_{int}(x,y), \{when\ x = p\} \quad (5)$$

$$I_{90}(r,\theta) = \sum_{x=1}^{m} f_{int}(x,y), \{when\ y = r\} \quad (6)$$

For size estimation, we use the peak of the area projection value, A_p that is the mean value of peaks of $A_0(p,\theta)$ and $A_{90}(r,\theta)$ in (3) and (4). $A_0(p,\theta)$ and $A_{90}(r,\theta)$ are the functions of p and r at the angel θ. Also, we use the peak value of the intensity projection, I_p that is the mean value of peaks of $I_0(p,\theta)$ and $I_{90}(r,\theta)$. In (5) and (6), $I_0(p,\theta)$ and $I_{90}(r,\theta)$ are the function of p and r also, but the integrating values are the intensity of the pixels.

C. *Size Estimation using Projection Parameters*

The size is estimated based on the models, S_1 and S_2, derived from empirical data. The models were established on the correlation between the size and the segmented ROI's number of pixels and intensity values. The relationship between the inclusion's size and the number of pixels in ROI was modeled for the size estimation parameter, S_1. S_1 is computed by the model based on the peak diameter versus sizes shown in (7). $a_0$and a_1 in (7) are defined by the empirical model. S_2 is found by the intensity and size relationship 2D linear regression model in (8). $b_0$and $b_1$in (8) are also obtained from the empirically developed model. This parameter is adapted due to the variation of surrounding tissues. We can capture the general sensor interaction ratio to the various conditions of tissue when the maximum force is applied. The final size, *S* is determined by the mean of the S_1 and S_2 values.

$$S_1 = a_0 (A_p - a_1) \quad (7)$$

$$S_2 = b_0 (I_p - b_1) \quad (8)$$

III. Experiments and Result

A. *Phantom Experimental Setup*

The phantom experimental setups are shown in Figure 5. The sensing device is SCIS v.1 with iPhone 6. The brightness of the sensor fixed at level 2 and the camera

exposure time at 0.067secs, sensitivity at 37. The experimental setup consists of four breast tissue mimicking layers made by PVC. Base layer represents the firm chest structure with some tissue in a human breast which has elasticity 124 ± 5kPa. The intermediate and depth layer simulate the main breast tissue which has 7 ± 1kPa elasticity. The tough and clear protective layer emulates the surface skin with 78 ± 3kPa elasticity.

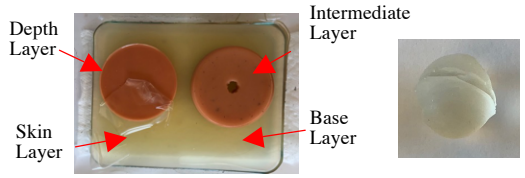

(a) (b)

Figure 5. Experimental setup (a) and PDMS tumor phantom (b)

The inclusion of phantom is shown in Figure 5(b). For the different size inclusion test, we used 8.00mm, 9.0mm, 12.0mm, 13.7mm, 15.6mm, and. 18.0mm hard inclusion. 17.0mm and hardness scale in Shore OO-10, 42, 50, 55, 65, and 95 inclusion phantoms were used for data acquisition of the various hardness with one size. *In vivo* data from four female breast cancer patients were also collected..

B. Phantom and Human Data Result

The proposed projection method has been tested with the phantoms and human patients. The phantom testing result consists of two parts; 5-different size inclusion test and 6-different hardness test for 17mm size inclusion. The varying size estimation resulted in 7.59% error for 2mm depth phantom and 14.58% error for 10mm depth case as shown in Table I. For the result of inclusions with varying hardness (in Table II), the size errors were 9.16% when the inclusion embedded in 2mm depth tissue and 24.70% for 10mm depth.

TABLE I. SIZE ESTIMATION EXPERIMENTAL RESULT - VARYING SIZE PHANTOM DATA; SOLID SPHERICAL OBJECTS, SIZES: $9.00mm, 12.0mm, 13.7mm, 15.6mm$, AND $18.0mm$

True Size (mm)	*Estimated Size (mm)*	*Error (%)*	*Estimated Size (mm)*	*Error (%)*
	2mm Depth		*10mm Depth*	
9.00	8.66	3.75	7.01	22.16
12.00	11.58	3.48	10.18	15.17
13.70	12.69	7.40	10.76	21.50
15.60	16.15	3.50	16.68	6.90
18.00	21.57	19.84	19.29	7.18
Average Error (%)	7.59		14.58	

TABLE II. EXPERIMENTAL RESULT –$17.0mm$VARYING HARDNESS PHANTOM DATA; SHORE HARDNESS OO-10, 42, 50, 55, 65, 95

	Size Estimation Error %			
Depth	2mm		10mm	
Shore OO Hardness	Projection Method	3D Interpolation Method	Projection Method	3D Interpolation Method
10	13.52	34.01	43.25	41.02
42	7.29	18.18	10.85	44.09
50	5.59	22.20	36.68	33.28
55	8.58	6.64	22.72	24.09
65	5.29	19.22	18.94	27.05
95	14.70	6.50	15.77	33.89
AVE (%)	**9.16**	**17.79**	**24.70**	**33.90**

The human data's size estimation using projection resulted in 23.05% error. The 3D interpolation method gave 56.03% error. So, the new projection method improved the size estimation by 58.9%.

TABLE III. EXPERIMENTAL RESULT –HUMAN DATA

Case	Ultrasound Size Measurement, Max Length	Depth	SCIS Measurement, Error %	
			3D interpolation Method	Projection Method
1	15.4mm	10.0mm	67.98	20.03
2	15.0mm	7.0mm	36.05	20.74
3	11.0mm	15.0mm	58.19	41.69
4	18.0mm	2.0mm	61.91	9.72
	Average error %		56.03	23.05

IV. CONCLUSION

SCIS is a system that helps early detection of breast tumor by estimating the mechanical properties. By using area projection of SCIS image, the size errors were 9% to 24% for phantoms and about 23% for humans. This corresponds to over 58% improvement over previous 3D interpolation method. Integrating a smartphone technology reduced the hardware cost while the accessibility increased for the women in the less developed country and women in remote regions.

REFERENCES

[1] Siegel, R. L., Miller, K. D., & Jemal, A. (2019). Cancer statistics, 2019. CA: A Cancer Journal for Clinicians, 69(1), 7–34. https://doi.org/10.3322/caac.21551

[2] "Cancers", (Sep, 2018). World Healthy Organization. [online] retrieved from: https://www.who.int/news-room/fact-sheets/detail/cancer

[3] M.O. Coleman, et al. (2008). Cancer survival in five continents: a worldwide population-based study (CONCORD). Lancet Oncol, 9, 730–56.

[4] C.-H. Won, Temple University of the Common Wealth of Pennsylvania, "Apparatus and method for surface and subsurface tactile sensation imaging," U.S. Patent No. 9652696, May 16, 2017.

[5] Oleksyuk, V., Rajan, R., Saleheen, F., Caroline, D., Pascarella, S., & Won, C. (2018). Risk Score Based Pre-Screening of Breast Tumor Using Compression Induced Sensing System. IEEE Sensors Journal, 18, 4038-4045.